Quantitative Finance

ISSN: (Print) (Online) Journal homepage: www.tandfonline.com/journals/rquf20

Assessing network risk with FRM: links with pricing kernel volatility and application to cryptocurrencies

Ruting Wang, Valerio Potì & Wolfgang Karl Härdle

Quantitative Finance, 2024
Vol. 24, No. 7, 975–992, https://doi.org/10.1080/14697688.2024.2370311

Assessing network risk with FRM: links with pricing kernel volatility and application to cryptocurrencies

RUTING WANG†, VALERIO POTÌ*‡ and WOLFGANG KARL HÄRDLE§¶‖**††‡‡

†Business School, Sun Yat-sen University, Shenzhen, People's Republic of China
‡Smurfit Graduate Business School, University College Dublin, Dublin, Ireland
§IRTG 1792, Humboldt-Universität zu Berlin, Berlin, Germany
¶Wang Yanan Institute for Studies in Economics, Xiamen University, Xiamen, People's Republic of China
‖Sim Kee Boon Institute for Financial Economics, Singapore Management University, Singapore, Singapore
**Faculty of Mathematics and Physics, Charles University, Prague, Czech Republic
††Yushan Scholar, National Yang Ming Chiao Tung University, Hsinchu, Taiwan
‡‡IDA Institute for Digital Assets, Bucharest University of Economic Studies, Bucharest, Romania

(*Received 18 October 2023; accepted 30 May 2024*)

The Financial Risk Meter (FRM) employs Quantile-LASSO regression to identify systemic financial risk and dependencies among tail events across financial assets. This paper establishes, both theoretically and empirically, a meaningful economic relationship between the FRM index, derived from the penalization parameter in quantile LASSO regression, and the volatility of assets' pricing kernels, the attainable maximal Sharpe ratio, and market volatility. Despite the rapid growth of the crypto market and its increasing integration with traditional financial markets, there remains a dearth of risk measures in this space. *FRM@Crypto* exhibits robust predictive capabilities in anticipating future market risk, potentially filling a critical void in this market.

Keywords: Network dynamics; Quantile LASSO regression; Market risk; Regularisation; Penalisation parameter; Cryptocurrencies

JEL Classification: G14, G17, C58

1. Introduction

The basic element of the FRM methodology is the CoVaR risk measure developed by Adrian and Brunnermeier (2016). CoVaR measures the stress level of a defined node (e.g. a financial institution) in a network given that another node (e.g. another financial institution) is at risk. FRM exploits this idea while allowing for either all or a subset of nodes to be at risk and it is based on the TENET risk measure of Härdle *et al.* (2016) and Fan *et al.* (2018), which combines CoVaR with a network model of risk exposures.

In its essence, the FRM is an average over the optimal Lagrangian parameters in a Quantile LASSO Regression, as explained for example by Mihoci *et al.* (2020). FRM is a multifunctional tool capable of assessing both the tail risk at the market level and the dynamic risk contagion between different assets within the market. Before the present application to cryptocurrencies, it has been applied to equity markets in America, Europe, and Asia, as well as in other developed and emerging markets. The up-to-date FRM indices are available online at frm.wiwi.hu-berlin.de.

On May 22, 2010, the first significant retail transaction involving Bitcoin and physical goods occurred when 10,000 mined Bitcoin were exchanged for two pizzas from a local pizza restaurant in Florida.† Then, after years of obscurity, Bitcoin saw a massive bull market in 2017-2018 that propelled its price to an all-time high of $66,002.23 in October 2021, according to Coinmarketcap. This corresponded to a

*Corresponding author. Email: valerio.poti@ucd.ie

† https://en.wikipedia.org/wiki/History_of_bitcoin

surge of interest that sparked an explosion in the offering of new cryptocurrencies. Today, the cryptocurrency market boasts more than 22,163 tradable cryptocurrencies, with a total market capitalization exceeding $1.1 trillion. The rapid growth of the cryptocurrency market is positioning it to play an increasingly pivotal role in the broader financial system. Though once ignored, cryptocurrencies like Bitcoin are now demanding attention as this emerging asset class continues to expand its influence.

Research has examined interconnectedness and contagion effects between cryptocurrencies, as well as between cryptocurrency and traditional financial markets. One strand focuses on the downside risk contagion between different cryptocurrencies. Borri (2019) showed that crypto-assets are highly exposed to tail risk from crypto markets but not from traditional assets. Building on this, Ahelegbey *et al.* (2021) examined relationships between crypto assets during stressful times using two econometric modeling techniques for measuring tail risk: extreme downside hedge (EDH) and extreme downside correlation (EDC). They found cryptocurrencies can be clustered into two groups: Speculative assets like Bitcoin that are mainly ‘givers’ of tail contagion and technical assets like Ethereum that are mainly ‘receivers’ of contagion. Giudici *et al.* (2022) utilized a spillover modeling methodology to evaluate the contagion effect amongst basket currencies and concludes that a stablecoin pegged to a basket of currencies exhibits lower volatility than all single currencies. The second strand explored the correlations between cryptocurrencies and conventional financial markets. Klein *et al.* (2018) used a BEKK-GARCH model to confirm flight-to-quality from Bitcoin to gold in times of crisis, questioning Bitcoin’s ‘virtual gold’ role. However, GARCH-based models are limited in only capturing average correlations, missing information about the whole distribution, especially the tails. Other studies have also uncovered downside risk spillover effects between Bitcoin and traditional assets using pairwise correlation analysis (Feng *et al.* 2018, Shahzad *et al.* 2019, 2020). Jiang *et al.* (2022) expanded on this work by quantifying the complex network effects. Their work instead concentrated on left-tail risk spillovers rather than average volatility spillovers between Bitcoin and traditional assets. However, despite evidence of tail risk contagion between crypto and traditional markets, rigorous mathematical arguments and empirical evidence connecting tail-event contagion to broad market risk in a clear-cut way are still lacking. The discussion of risk interconnectedness within the FinTech market extends beyond cryptocurrencies. Giudici *et al.* (2019) advance credit risk assessments on peer-to-peer lending platforms by embedding the topological data into similarity networks, which are derived from the financial information of borrowers. In the context of these research endeavors, the present article makes two major contributions.

First, our study expands existing work on the FRM by providing a deeper economic interpretation of the risk index. Supported by simulation based empirical tests, Zbonakova *et al.* (2017) show that the index depends on three major factors: the variance of the error term, the correlation structure of the covariates and the number of non-zero coefficients of the asset return model used in the construction of the index. Ren *et al.* (2022) and Wang *et al.* (2023) further extend the analysis by adding a Lagrange multiplier interpretation. Building on their analysis, this work offers both empirical and analytical evidence of the connection between the FRM index and the volatility of the pricing kernel. This way, we contribute to the literature (e.g. Kozak *et al.* 2020, Chen and Potì 2024) that is establishing a connection between optimal measures of regularization in regressions of asset returns and the volatility of the kernel that prices the assets.

Second, our study demonstrates that FRM carries forward-looking information for risk in cryptocurrencies. This can be very useful in managing cryptocurrency risk because, for many (though not all)† cryptocurrencies, option markets are still underdeveloped and less mature in comparison to other assets. For such cryptocurrencies, forward-looking information about risk provided by option markets is harder to obtain and in some cases unavailable.‡ Therefore, in such situations, the forward-looking risk information offered by FRM becomes even more valuable.

In this paper, we examine the dependencies among tail events (TE) in cryptocurrency markets as well as constructing a novel market risk measure through the utilization of the FRM framework (Härdle *et al.* 2016), which is based on the TENET Quantile LASSO Regressions. In the theoretical part, we provide an interpretation of the lasso penalty parameter λ based on the properties of Lagrangian multiplier. We then elucidate its relationship with the spread between the in-sample and the out-of-sample asset return predictability, the pricing kernel’s volatility and the maximal attainable Sharpe ratio, as well as its association with market volatility. In the empirical section, we demonstrate how to compute the market risk index *FRM@Crypto* by averaging the penalty parameters from each regression for individual cryptocurrencies. Our initial analysis focuses on evaluating the ability of *FRM@Crypto* to forecast future market volatility and returns. Our analysis reveals that *FRM@Crypto* predictively accounts for 63.8–76.6% of out-of-sample market volatility. In addition, a comparison with other commonly utilized risk measures demonstrates that *FRM@Crypto* outperforms in predicting market volatility over a horizon of up to 5 weeks. We also highlight its capacity to explain Sharpe ratio volatility, thereby reinforcing the empirical support for the properties of FRM that we demonstrate in our theoretical analysis. To assess if *FRM@Crypto* can mitigate losses in portfolio construction, we integrate FRM into a portfolio construction approach that builds on the Markowitz framework. Our analysis shows that by incorporating FRM into the portfolio construction process, we can create a portfolio that withstands extreme market movements (tail events) effectively. Additionally, when examining the ‘co-stress’ coefficients within the cryptocurrency market network, we find a negative correlation between closeness centrality and *FRM@Crypto*. In contrast, there is a positive correlation between eigenvector centrality and *FRM@Crypto*.

† Deribit, founded in 2016, has emerged as the largest exchange for cryptocurrency options. It has deep liquidity, similar to traditional options markets, yet the underlying assets of the options traded on this market include only a fraction of the large set of cryptocurrencies that exist.

‡ The risk-neutral distribution that prices the options reflects, under a change of measure, the option market participants’ beliefs about the distribution of the underlying asset. In the absence of quoted or traded prices for liquid option contracts, the calculation of such risk-neutral distribution presents greater challenges and the result might not be at all meaningful.

The structure of the remainder of the paper is as follows: Section 2 provides an overview of the FRM construction methodology; Section 3 delves into the economic interpretation of the regularization parameter, highlighting its significance in capturing the spread between in-sample and out-of-sample predictability of asset returns, thus between in-sample and out-of-sample pricing kernel volatility and Sharpe ratios; Section 4 presents empirical evidence supporting the theoretical analysis using cryptocurrency market data; Section 5 scrutinizes risk contagion within the network of cryptocurrencies; Finally, Section 6 summarizes our findings. Tables and figures are in the appendix.

All the underlying code is available as quantlets through www.quantlet.de and the corresponding results are marked with a sign, which serves as a link. The courselet on FRM@Crypto is available at www.quantinar.com .

2. The FRM construction

FRM's fundamental framework is developed from CoVaR (Adrian and Brunnermeier 2016). The FRM uses quantile regression to capture cryptocurrencies' TE risk transmission and market risk. Linear quantile lasso regression for log return series $r_{j,t}$ in a window of k days is given by

$$r_{j,t} = \alpha_j + A_{j,t}^\top \beta_j + \varepsilon_{j,t}, \quad j \in \{1, 2, \dots, N\} \tag{1}$$

with N cryptocurrencies and m macro-state variables. $A_{j,t}^\top \overset{def}{=} [M_{t-1}, r_{-j,t}]$ represents a $p = N + m - 1$ dimensional vector of covariates and $t \in \{1, \dots, k\}$. $r_{-j,t}$ is the daily log return of all the cryptocurrencies except the jth cryptocurrency on day t. M contains the macroeconomic variables on day $t-1$. β_j is a $p \times 1$ vector.

The estimated coefficients are obtained by performing the minimization in equation (2) for each rolling window k, with ℓ_1-norm penalization, lasso parameter λ_j, and loss function ρ_τ.

$$\hat{\beta}_\tau = \arg\min_{\beta_j} \mathsf{E}_{X_j, A_j} \left\{ \rho_\tau \left(r_j - \alpha_j - A_j \beta_j \right) \right\} \tag{2}$$

where the quantile level τ represents the probability of tail events (in the main part of our analysis, we set $\tau = 5\%$) and the quantile loss function here is defined as:

$$\rho_\tau(u) = |\tau - \mathbf{I}\{u \le 0\}||u| \tag{3}$$

To reduce the variance of the estimator $A_j^\top \beta_j$, the problem is regularized under the ℓ_1-norm, according to Tibshirani (1996), thus becoming a Quantile LASSO regression. That is, equation (2) is supplemented with the constraint $\| \beta_j \|_1 \le b$. The constraint level b is optimized so that it minimizes the objective expected loss function over all possible levels:

$$b^* = \arg\min_b \mathsf{E}_{r_j, A_j} \left[\rho_\tau \left\{ r_j - \alpha_j - A_j \beta_\tau(b) \right\} \right] \tag{4}$$

Thus, the overall task can be summarized as a consecutive three-fold extrema search:

$$\min_b \max_{\lambda_j} \min_{\beta_j} \left\{ \mathsf{E}_{r_j, A_j} \left(\rho_\tau \left[r_j - \alpha_j - A_j \beta_j \left\{ \lambda_j(b) \right\} \right] \right) + \lambda_j(b) \parallel \beta_j \left\{ \lambda_j(b) \right\} \parallel_1 \right\} \tag{5}$$

Letting at each time point $t \in 1 : T$ logarithmic returns $r_{t,j}$ of cryptocurrency $j \in 1 : J$ constitute the response variables for the quantile regressions, the optimal λ_j according to GACV is thus defined as:

$$\min_{\lambda_j} \mathrm{GACV}(\lambda_j) = \min_{\lambda_j} \frac{\sum_{t=1}^{k} \rho_\tau \{ r_{j,t} - \alpha_{j,t} - A_{j,t}^\top \beta_j(\lambda_j) \}}{n - \mathrm{tr}\{S(\lambda_j)\}} \tag{6}$$

The FRM daily index is then defined as:

$$\mathrm{FRM} \overset{\mathrm{def}}{=} \frac{1}{N} \sum_{j=1}^{N} \lambda_j \tag{7}$$

The standard FRM index for each trading day is calculated as the average of the penalty parameters from Quantile LASSO regressions, which are estimated based on the past 3-month rolling-window of data. The evolution of averaged λ_j represents the variation of the systemic tail risks (Härdle *et al.* 2016, Mihoci *et al.* 2020, Ren *et al.* 2022). Thus, the FRM index measures joint tail events.

3. The FRM interpretation

3.1. *Shadow price from the perspective of lagrangian multiplier*

The convex programing problem that quantile LASSO solves is as follows:

$$\begin{aligned} &\min_\beta \mathsf{E}_{r_j, A_j} \left\{ \rho_\tau \left(r_j - \alpha_j - A_j^\top \beta_j \right) \right\} \\ &\text{s.t.} \ \parallel \beta_j \parallel_1 \le b \end{aligned} \tag{8}$$

If we denoted the expected gain $R(\beta) = -\mathsf{E}_{r_j, A_j} \{ \rho_\tau (r_j - \alpha_j - A_j^\top \beta_j) \}$, and the constraint function $B(\beta_j) = \parallel \beta_j \parallel_1$, the Lagrangian formulation of the optimization objective in equation (8) is:

$$\mathcal{L}(\beta_j, \lambda_j) = R(\beta_j) - \lambda_j \left\{ B(\beta_j) - b \right\}$$

To find the optimum, one can turn to the Karush–Kuhn–Tucker (KKT) conditions:

$$\nabla_{\beta_j, \lambda_j} \mathcal{L}(\beta_j^*, \lambda_j^*) = 0 \tag{9}$$

If one views the Lagrangian $\mathcal{L}\{\beta_j(b), \lambda_j(b), b\}$ as a function of the budget constraint b, the Lagrangian multiplier λ_j becomes a derivative with respect to b when evaluated at the solution $\{\beta_j^*(b), \lambda_j^*(b)\}$, due to KKT conditions equation (9) and the chain rule:

$$\begin{aligned} \frac{d}{db} \mathcal{L} \left\{ \beta_j^*(b), \lambda_j^*(b), b \right\} &= \underbrace{\frac{d\mathcal{L}}{d\beta_j}}_{=0} \frac{d\beta_j^*}{db} + \underbrace{\frac{d\mathcal{L}}{d\lambda_j}}_{=0} \frac{d\lambda_j^*}{db} + \frac{d\mathcal{L}}{db} \\ &= \lambda_j^*(b) \end{aligned} \tag{10}$$

Furthermore, note that at the optimal value the Lagrangian equals the expected gain R:

$$\mathcal{L}(\beta_j^*, \lambda_j^*, b) = R(\beta^*) - \lambda_j^* \underbrace{\{B(\beta_j^*) - b\}}_{=0} = R^*(b) \qquad (11)$$

Combing equations (10) and (11), we see that we can regard λ_j as the rate of change of the expected gain with respect to the budget constraint:

$$\lambda_j^*(b_0) = \left.\frac{dR^*}{db}\right|_{b=b_0} \qquad (12)$$

This holds for cases of both positive and zero λ_j.

When considering a regression model as a predictive tool, the value of λ_j can be seen as a *shadow price*, reflecting the impact on the model's predictive power of loosening the budget constraint imposed by limiting the size of the model parameters. In other words, λ_j represents the additional predictive gain obtained from relaxing this constraint by a small amount, and is thus referred to as the *marginal predictability gain*.

3.2. FRM's relation with market volatility and pricing kernel volatility

We next illustrate the relation between the FRM index, the volatility of pricing kernels and the maximal attainable Sharpe ratio in the context of the simpler special case in which FRM is obtained from linear LASSO regressions. The extension to the quantile case is considered in Appendix A.1. This section is inspired by Kirby (1998), Potì and Wang (2010), Huang and Zhou (2017), Potì (2018), Kozak *et al.* (2020), Korsaye *et al.* (2021) and Chen and Potì (2024).

In the absence of arbitrage opportunities, as discussed in Cochrane (2009), the following relationship holds for the conditional expectation under the real-world (physical) measure denoted as P:

$$\mathsf{E}^{\mathrm{P}}_{\mathcal{F}_t}[m_{t+1}R_{j,t+1}] = 1 \qquad (13)$$

Here, the filtration $\mathcal{F}_t$ represents the information available up to time t for the investors with rational expectations (RE), $m_{t+1} > 0$ represents a pricing kernel (stochastic discount factor), and $R_{j,t+1}$ is the return on asset j adapted to the filtration $\mathcal{F}_t$, with $R_{j,t+1} \stackrel{\text{def}}{=} \frac{x_{j,t+1}}{x_{j,t}}$, where $x_{j,t}$ denotes the asset payoff at time t (hence, following the convention in the asset pricing literature, by return we mean the ratio of next period payoff to the current period payoff which, by no-arbitrage, must coincide with the current price), $j = 1, \dots, N$, where N is the number of tradable assets. Since, in general, m_{t+1} is not unique, we refer here to the least volatile (minimum-variance) one. In this setup, $m_{t+1} > 0$ is therefore the minimum-variance kernel or stochastic discount factor that prices the asset returns under the probability distribution, P, embodying beliefs of a marginal investor endowed with RE, hence the objective physical measure.

Denoting excess-returns as $r_{j,t+1} \stackrel{\text{def}}{=} R_{j,t+1} - r_t^f - 1$, where r_t^f is the risk-free rate, we can rewrite equation (13) as follows:

$$\mathsf{E}^{\mathrm{P}}_{\mathcal{F}_t}[(1 + r_t^f + r_{j,t+1})\, m_{t+1}] \approx 1 \qquad (14)$$

Applying equation (13) to the return on risk-free asset, $1 + r_t^f \approx 1$, we have that

$$\mathsf{E}^{\mathrm{P}}_{\mathcal{F}_t}[m_{t+1}] = \frac{1}{(1 + r_t^f)} \approx 1 \qquad (15)$$

Based on the law of one price (implied by the no-arbitrage assumption), we can combine equations (14) and (15) and obtain the following expression:

$$\mathsf{E}^{\mathrm{P}}_{\mathcal{F}_t}[m_{t+1}r_{j,t+1}] \approx 0 \qquad (16)$$

Taking unconditional expectations of both sides of equation (15), one arrives at

$$\mathsf{E}^{\mathrm{P}}[m_{t+1}] \approx 1 \qquad (17)$$

Similarly, taking unconditional expectations of both sides of equation (16), one gets

$$\mathsf{E}^{\mathrm{P}}[m_{t+1}r_{j,t+1}] \approx 0 \qquad (18)$$

Hence,

$$\underbrace{\mathsf{E}^{\mathrm{P}}[m_{t+1}]}_{\approx 1} \mathsf{E}^{\mathrm{P}}[r_{j,t+1}] + \mathrm{Cov}[m_{t+1}, r_{j,t+1}] \approx 0$$

Therefore,

$$\mathsf{E}^{\mathrm{P}}[r_{j,t+1}] \approx -\underbrace{\mathrm{Corr}[m_{t+1}, r_{j,t+1}]}_{\in[-1,1]} \sigma(m_{t+1})\, \sigma(r_{j,t+1}) \qquad (19)$$

Under the real-world (physical) measure, $\mathrm{Cov}[m_{t+1}, r_{j,t+1}]$ represents the covariance between the pricing kernel and the return of asset j at time $t+1$, while $\mathrm{Corr}[m_{t+1}, r_{j,t+1}]$ denotes the correlation between them. Also, $\sigma(\mathrm{m}_{t+1})$ and $\sigma(\mathrm{r}_{j,t+1})$ represent the standard deviations of the pricing kernel and the return of asset j at time $t+1$, respectively.

Under the empirical distribution, the approximate equation in equation (19) still holds:

$$\widehat{\mathsf{E}}^{\mathrm{P}}[r_{j,t+1}] \approx -\underbrace{\widehat{\mathrm{Corr}}[m_{t+1}r_{j,t+1}]}_{\in[-1,1]} \hat{\sigma}(m_{t+1})\, \hat{\sigma}(r_{j,t+1}) \qquad (20)$$

Here, $\widehat{\mathsf{E}}^{\mathrm{P}}[r_{j,t+1}]$ represents an in-sample estimate of expected return, while $\widehat{\mathrm{Corr}}[m_{t+1}r_{j,t+1}]$, $\widehat{\sigma}(m_{t+1})$ and $\widehat{\sigma}(r_{j,t+1})$ are in-sample estimates of the correlation between the pricing kernel and the asset's excess return, along with their standard deviations, respectively.

Subtracting equations (20) from (19), we have:

$$\mathsf{E}^{\mathrm{P}}[r_{j,t+1}] - \widehat{\mathsf{E}}^{\mathrm{P}}[r_{j,t+1}] \approx \underbrace{\widehat{\mathrm{Corr}}[m_{t+1}r_{j,t+1}]}_{\in[-1,1]} \hat{\sigma}(m_{t+1})\, \hat{\sigma}(r_{j,t+1})$$

$$- \underbrace{\mathrm{Corr}[m_{t+1} r_{j,t+1}]}_{\in[-1,1]} \sigma(m_{t+1})\, \sigma(r_{j,t+1}) \tag{21}$$

If we disregard the sampling errors of $\widehat{\mathrm{Corr}}[m_{t+1} r_{j,t+1}]$ and $\widehat{\sigma}(r_{j,t+1})$, equation (21) can be rewritten as follows:†

$$\mathsf{E}^{\mathrm{P}}[r_{j,t+1}] - \widehat{\mathsf{E}}^{\mathrm{P}}[r_{j,t+1}] \approx \underbrace{\mathrm{Corr}[m_{t+1} r_{j,t+1}]}_{\in[-1,1]} \sigma(r_{j,t+1}) \times [\widehat{\sigma}(m_{t+1}) - \sigma(m_{t+1})] \tag{22}$$

By the Cauchy inequality, we thus have:

$$|\mathsf{E}^{\mathrm{P}}[r_{t+1,k}] - \widehat{\mathsf{E}}^{\mathrm{P}}[r_{j,t+1}]| \le \sigma(r_{j,t+1}) |\widehat{\sigma}(m_{t+1}) - \sigma(m_{t+1})| \tag{23}$$

The in-sample estimated expected return ($\widehat{\mathsf{E}}^{\mathrm{P}}[r_{j,t+1}]$) in equation (23) can be modeled using the OLS estimate of the regression in equation (1), denoted as $\mathsf{E}_n^{\mathrm{OLS}}[r_{j,t+1}]$. A consistent estimate of $\mathsf{E}^{\mathrm{P}}[r_{t+1,k}]$ is instead provided by $\mathsf{E}_n^{\mathrm{CV}}[r_{j,t+1}]$, where $\mathsf{E}_n^{\mathrm{CV}}[.]$ represents the cross-validation estimate of the FRM regression.‡ Thus, equation (23) can be rewritten as follows:

$$|\mathsf{E}_n^{\mathrm{CV}}[r_{j,t+1}] - \mathsf{E}_n^{\mathrm{OLS}}[r_{j,t+1}]| \le \sigma(r_{j,t+1}) |\hat{\sigma}(m_{t+1}) - \sigma(m_{t+1})| \tag{24}$$

Moreover, denoting the ex-ante Sharpe ratio ('Sharpe ratio' for short) as $Sharpe_j = \frac{\mathsf{E}^{\mathrm{P}}[r_{j,t+1}]}{\sigma(r_{j,t+1})}$ and recalling the well-known duality between pricing kernel volatility and the attainable maximal Sharpe ratio (Hansen and Jagannathan 1991), we get the following additional insight based on equation (19):

$$Sharpe_j = \frac{\mathsf{E}^{\mathrm{P}}[r_{j,t+1}]}{\sigma(r_{j,t+1})} \approx - \underbrace{\mathrm{Corr}[m_{t+1}, r_{j,t+1}]}_{\in[-1,1]} \sigma(m_{t+1}) \tag{25}$$

$$\max(Sharpe_j) = \sigma(m_{t+1}) \tag{26}$$

$$|\mathsf{E}_n^{\mathrm{CV}}[r_{j,t+1}] - \mathsf{E}_n^{\mathrm{OLS}}[r_{j,t+1}]| \le \sigma(r_{j,t+1}) |\max(\widehat{Sharpe_j}) - \max(Sharpe_j)| \tag{27}$$

This leads to the following proposition.

PROPOSITION 3.1 *In the absence of arbitrage opportunities, λ_j is proportional to both the asset volatility and the absolute value of the spread between the minimum-variance kernels that price the assets in-sample and ex-ante. That is,* $\forall j$

$$\begin{aligned} \lambda_j &\propto \sigma(r_{j,t+1}) \\ \lambda_j &\propto \left|\hat{\sigma}(m_{t+1}) - \sigma(m_{t+1})\right| \\ \lambda_j &\propto \left|\max(\widehat{Sharpe_j}) - \max(Sharpe_j)\right| \end{aligned} \tag{28}$$

† $\widehat{\mathrm{Corr}}[m_{t+1} r_{j,t+1}] \widehat{\sigma}(r_{j,t+1}) \approx \mathrm{Corr}[m_{t+1} r_{j,t+1}]_{\in[-1,1]} \sigma(r_{j,t+1})$.
‡ The details of the mathematical argument are provided in Appendix A.2.

Proof The existence of m_t is guaranteed under the assumption that the law of one price holds (implicitly assumed when assuming $m_{t+1} > 0$) whereas the existence of $\widehat{m}_t$ is trivially guaranteed by the weak stationarity assumption (which guarantees finite variances). The magnitude of the left-hand side of equation (24) depends on λ_j since the greater the value of λ_k, the larger the value on the left-hand side of equation (24). Thus, $\lambda_j \propto |\mathsf{E}_n^{\mathrm{CV}}[r_{j,t+1}] - \mathsf{E}_n^{\mathrm{OLS}}[r_{j,t+1}]|$.§ Consequently, the right-hand side of the equation is also proportional to λ_j. That is,

$$\lambda_j \propto \sigma(r_{j,t+1})\, |\widehat{\sigma}(m_{t+1}) - \sigma(m_{t+1})| \tag{29}$$

Hence, keeping $|\widehat{\sigma}(m_{t+1}) - \sigma(m_{t+1})|$ constant,

$$\lambda_j \propto \sigma(r_{j,t+1}) \tag{30}$$

Similarly, keeping $\sigma(r_{j,t+1})$ constant,

$$\lambda_j \propto |\widehat{\sigma}(m_{t+1}) - \sigma(m_{t+1})| \tag{31}$$

$$\lambda_j \propto \left|\max(\widehat{Sharpe_j}) - \max(Sharpe_j)\right| \tag{32}$$

■

REMARK 3.1 Due to the duality between volatility of the minimum variance pricing kernel and the maximal attainable Sharpe ratio attainable by investing in the N assets, λ_j is proportional to $|\widehat{\sigma}(m_{t+1}) - \sigma(m_{t+1})|$ and $|\max(\widehat{Sharpe_j}) - \max(Sharpe_j)|$.

REMARK 3.2 The following properties of λ_j can be derived from Remark 3.1:

(i) The positive relationship between λ_j and asset price volatility implies its contemporaneous correlation with risk measures.
(ii) λ_j is proportional to the spread between in-sample and (the unobservable) true pricing kernel volatility and maximal Sharpe ratios.

REMARK 3.3 As indicated by the expression in equation (7), the FRM is the average value of all the λ_j of LASSO regressions within the given network with N assets. Therefore, the FRM keep the essential properties of the individual λ_j.

4. Data and empirical design

4.1. Data description

We used price data from 62 cryptocurrencies available in the market, sourced from the Blockchain Research Center. For the dynamic construction of the tail-risk contagion network based on FRM and the calculation of the *FRM@Crypto* index, we employed data on the 15 largest cryptocurrencies on each trading day within rolling windows of 63 days. It is worth noting that at the beginning, only 8 highly liquid cryptocurrencies were in existence. As a result, we allowed the parameter J

§ Further discussion on this is given in Appendix A.3.

to remain dynamic until June 14, 2017, when the minimum requirement of $J = 15$ coins was first met. The total time span is from 1st June 2015 until the end of May 2022. Following the Adrian and Brunnermeier (2016), we also consider the impact of macro and macro-financial variables such as the US dollar index, the yield on USD Government T-Bill, the VIX, CVIX, and the S&P 500 index.

Table 1. Correlation between *FRM@Crypto* and variance of CRIX log return.

	FRM	Variance of CRIX log return
FRM		0.788***
Variance of CRIX log return	0.788***	

Note: ***, **, * denote significance at 1%, 5%, 10% level.

4.2. FRM and CRIX volatility

Yu *et al.* (2019) explored the relationship between FRM index and other well-established risk measures such as VIX and SRISK, in the context of the American stock market. However, given the absence of conventional risk measures for the cryptocurrency market, we compare *FRM@Crypto* with the 63-day rolling window variance of CRIX's returns. CRIX offered the first carefully constructed index of the cryptomarket (analogous to S&P 500), as detailed in Trimborn and Härdle (2018). The comparison is depicted in figure 1. It is noteworthy to observe the strong positive relation between *FRM@Crypto* and the 63-day variance of CRIX return. Table 1 shows that the Pearson correlation coefficient is 78.8%.

Increasing market volatility, which is measured as the rolling window variance of CRIX's price, signifies increased uncertainty in the out-of-sample prediction of returns, as well as a wider spread between in-sample and out-of-sample estimation outcomes. This strong correlation between *FRM@Crypto* and CRIX volatility aligns with $\lambda_j \propto |\mathsf{E}_n^{\text{CV}}[r_{j,t+1}] - \mathsf{E}_n^{\text{OLS}}[r_{j,t+1}]|$ and Proposition 3.1, particluarly with Remarks 3.2 and 3.3.

4.3. FRM's predictive power for price volatility and returns

According to Proposition 3.1, there exists a direct relationship between *FRM@Crypto* and the volatility of the cryptocurrencies' returns. To evaluate this assertion, we conduct regression analysis using lagged FRM as the independent variable and assess its relationship with both market volatility and return. We analyze both the in-sample and out-of-sample R^2. Furthermore, we conduct a comparative analysis of FRM's performance against other risk measures.

The market return is calculated as the market capitalization-weighted average of the daily returns of all cryptocurrencies. The risk measures (*Risk*) consist of FRM and four other measures described in Appendix A.3, namely the Bayesian Graphical VAR index (Ahelegbey *et al.* 2016), the Principal Components index (Billio *et al.* 2012), the Degree of Granger Causality index (Billio *et al.* 2012), and the Total Connectedness index (Diebold and Yilmaz 2012).

The regressions are specified as follows:

$$y_t^{\text{Market}} = \alpha + \beta_t Risk_{t-l} + \varepsilon_t \quad (33)$$

In the regression, we use as the dependent variable, y^{Market}, alternatively either the 63-day rolling average of the market return or, as an estimate of market volatility, its 63-day standard deviation. β_t is the coefficient of the risk measure. The term $Risk_{t-l}$ represents the risk measure calculated on day $t-l$, where l represents the number of lagged days.

Following Campbell and Thompson (2008), we compute in-sample and out-of-sample R^2 coefficients as follows, with

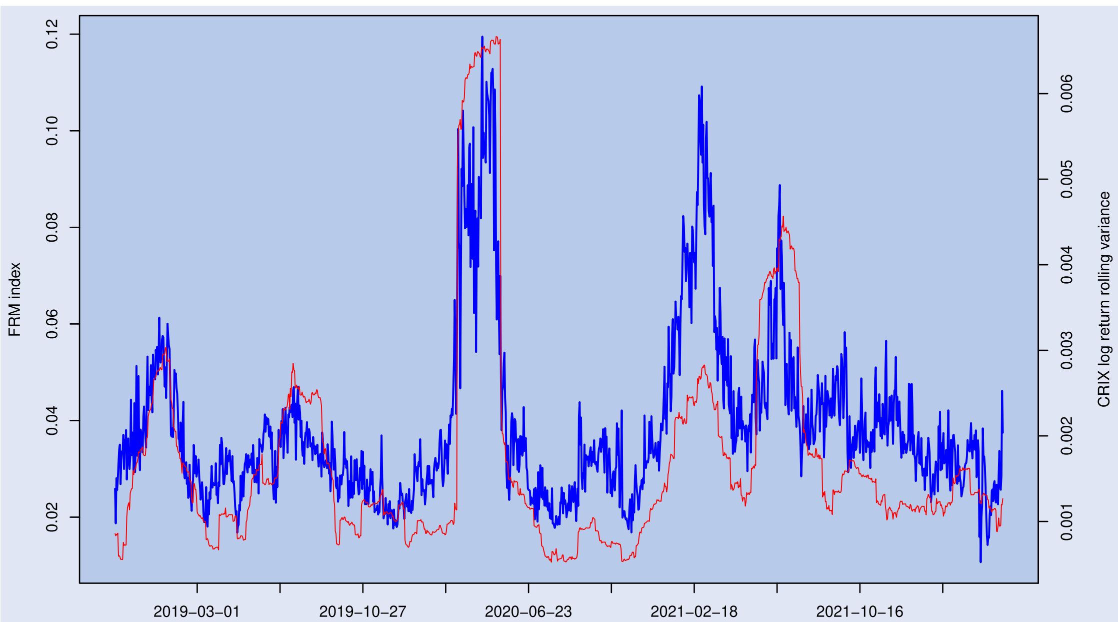

Figure 1. 5% FRM@Crypto and 63-day variance of CRIX log return.

Table 2. In-sample β of predictive regressions of market volatility on risk measures.

	10 days	5 weeks	3 months	5 months
FRM 5%				
β	0.5902***	0.5377***	0.2780***	0.1510***
Newey-West standard errors	0.027	0.031	0.033	0.035
FRM 25%				
β	1.0785***	1.0092***	0.5990***	0.3461***
Newey-West standard errors	0.051	0.052	0.059	0.057
FRM 50%				
β	0.6687***	0.6140***	0.3458***	0.2110***
Newey-West standard errors	0.032	0.033	0.038	0.039
Granger Causality				
β	0.0001	0.0027	− 0.0090	0.0056
Newey-West standard errors	0.015	0.017	0.020	0.020
Bayesian Graphical VAR				
β	0.0002	0.0004**	0.0008***	0.0005***
Newey-West standard errors	0.000	0.000	0.000	0.000
Principal Components				
β	0.0001***	0.0001***	0.0001	− 0.0000
Newey-West standard errors	0.000	0.000	0.000	0.000
Total Connectedness				
β	0.0002***	0.0002***	0.0001***	0.0001***
Newey-West standard errors	0.000	0.000	0.000	0.000

Note: ***, **, * denote significance at 1%, 5%, 10% level.

Table 3. In-sample and out-of-sample R^2 with $w = 63$ for crypto market's 63-day volatility regressed on risk indicators lagged with 10 days, 5 weeks, 3 months, and 5 months.

RHS	LHS	10 days	5 weeks	3 months	5 months
R^2					
FRM 5%	var	0.789	0.727	0.720	0.679
FRM 25%	var	0.747	0.699	0.635	0.649
FRM 50%	var	0.725	0.686	0.663	0.639
Bayesian Graphical VAR	var	0.739	0.700	0.664	0.725
Granger Causality	var	0.589	0.615	0.611	0.642
Principal Components	var	0.654	0.663	0.765	0.705
Total Connectedness	var	0.777	0.719	0.692	0.704
R^2_{OOS}					
FRM 5%	var	0.766	0.689	0.683	0.638
FRM 25%	var	0.722	0.668	0.601	0.611
FRM 50%	var	0.699	0.650	0.630	0.601
Bayesian Graphical VAR	var	0.701	0.666	0.632	0.697
Granger Causality	var	0.551	0.572	0.568	0.606
Principal Components	var	0.604	0.610	0.734	0.664
Total Connectedness	var	0.741	0.654	0.656	0.622

Table 4. In-sample and out-of-sample R^2 with $w = 63$ for crypto market's 63-day mean return regressed on risk indicators lagged with 10 days, 5 weeks, 3 months, and 5 months.

RHS	LHS	10 days	5 weeks	3 months	5 months
		R^2			
FRM 5%	return	0.554	0.634	0.611	0.615
FRM 25%	return	0.527	0.585	0.582	0.589
FRM 50%	return	0.538	0.596	0.586	0.587
Bayesian Graphical	return	0.556	0.596	0.603	0.610
Granger Causality	return	0.555	0.492	0.597	0.533
Principal Components	return	0.698	0.652	0.634	0.608
Total Connectedness	return	0.686	0.660	0.657	0.681
		R^2_{OOS}			
FRM 5%	return	0.504	0.594	0.560	0.574
FRM 25%	return	0.480	0.545	0.541	0.552
FRM 50%	return	0.491	0.557	0.541	0.548
Bayesian Graphical	return	0.504	0.555	0.560	0.573
Granger Causality	return	0.507	0.443	0.554	0.492
Principal Components	return	0.661	0.602	0.591	0.558
Total Connectedness	return	0.641	0.604	0.562	0.600

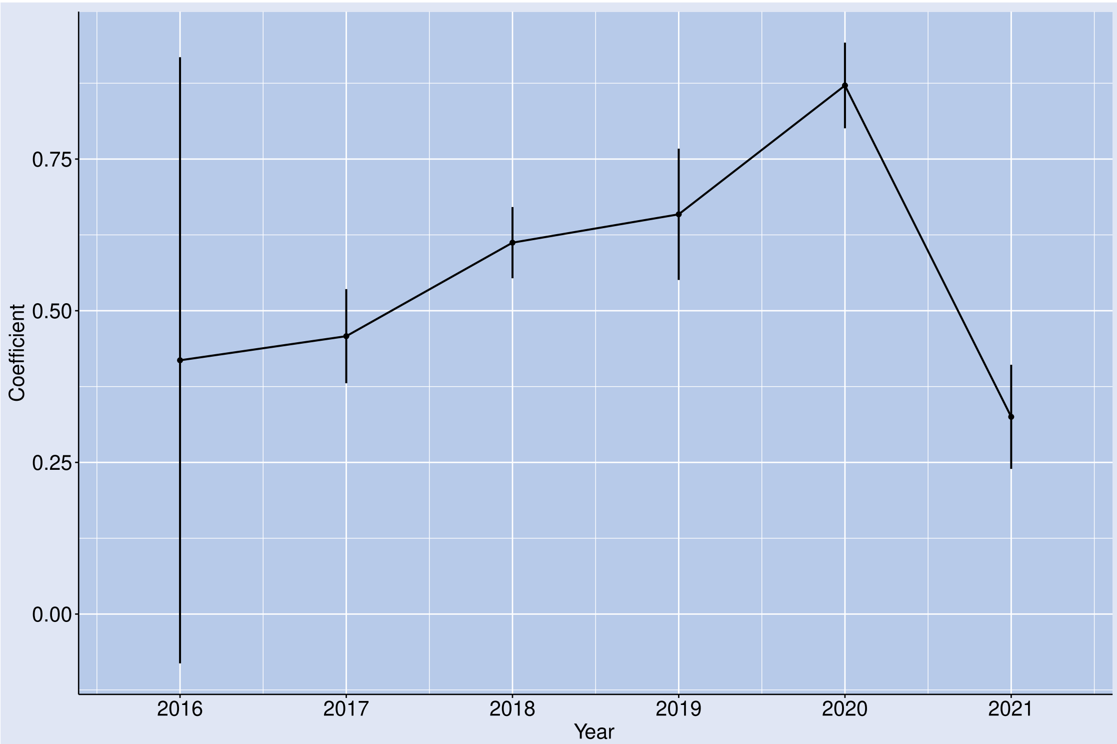

Figure 2. In-sample β and its 95% interval of regressions of market volatility on the 10-day lag of FRM ($\tau = 0.05$) estimated with non-overlapping yearly windows (one per year). The standard errors of the coefficients are calculated based on the Newey-West estimator.

a rolling estimation window ($w = 62$):

$$R^2 = 1 - \frac{\sum_{t=w}^{T-1} \left(y_{t+1} - \hat{y}_{t+1}\right)^2}{\sum_{t=w}^{T-1} \left(y_{t+1} - \bar{y}_{w+1}\right)^2} \quad (34)$$

$$R^2_{\text{OOS}} = 1 - \frac{\sum_{t=w}^{T-1} \left(y_{t+1} - \hat{y}_{t+1\,|\,t}\right)^2}{\sum_{t=w}^{T-1} \left(y_{t+1} - \bar{y}_{w+1}\right)^2} \quad (35)$$

Here, R^2 is the in-sample coefficient of determination and R^2_{OOS} is its out-of-sample counterpart; $\hat{y}_{t+1}$ is a linear prediction for $t+1$ based on observations from $t-w+2$ to $t+1$ ($\hat{y}_{t+1} = \hat{\beta}_{t+1} Risk_{t+1-l}$); $\hat{y}_{t+1\,|\,t}$ is a linear prediction for $t+1$ based on observations from $t-w+1$ to t ($\hat{y}_{t+1\,|\,t} = \hat{\beta}_t Risk_{t+1-l}$); $\bar{y}_{w+1} = (T-w)^{-1} \sum_{s=w+1}^{T} y_s$.

The results are shown in tables 2, 3 and 4. In table 2, we report and compare the in-sample estimates of the coefficient (β) of risk measures used as regressors of market volatility in predictive regressions like equation (33). According to these estimates, FRM with $\tau = 5\%$, $\tau = 25\%$, and $\tau = 50\%$ exhibits statistically significant positive relations

Table 5. In-sample and out-of-sample R^2 with $w = 63$ for market volatility regressed on itself lagged with 10 days, 5 weeks, 3 months, and 5 months.

	R^2				R^2_{OOS}			
RHS	10 days	5 weeks	3 months	5 months	10 days	5 weeks	3 months	5 months
var	0.8883	0.7201	0.7434	0.7143	0.7855	0.5556	0.681	0.5812

with future 10-day, 5-week, 3-month, and 5-month market volatility. To overcome autocorrelation and heteroskedasticity in the error terms in the models, we use the Newey-West estimator to adjust the standard error estimates. The results in tables 3 and 4 illustrate whether the FRM indexes with different τ perform well in predicting market volatility and return. The tables indicate that FRM demonstrates a stronger predictive capability for market volatility than for returns, especially when compared with other risk measures within the 5-week prediction horizon. This result supports Proposition 3.1 that *FRM@Crypto* is proportional to volatility. The *FRM@Crypto* has higher out-of-sample R^2 in market volatility prediciton than other indicators at both the 10-day and 5-week horizons. However, the Bayesian Graphical VAR and the Principal Component Index show slightly stronger predictive capabilities as the forecast horizon increases when horizon extends to 5 months.

We further regress market volatility on the 10-day lag of FRM ($\tau = 0.05$) over yearly non-overlapping estimation windows (one per year). The in-sample estimates of the β coefficient of these regressions and their 95% interval are depicted in figure 2. It is evident that the β of FRM ($\tau = 5\%$) in each year's sample is consistently and significantly positive.

To determine if the predictive capacity of FRM stems from capturing the persistence of the market volatility, we conduct regressions of the market volatility on its own lagged values. The outcomes are presented in table 5. As can be observed therein, while the predictive capability of lagged volatility is relatively strong, it does not outperform either FRM or the other alternative risk predictors. This implies that each predictor captures predictability in market volatility beyond its inherent persistence.

In Appendix A.3, We detail and present the findings from a series of robustness tests concerning the predictive effectiveness of FRM in forecasting future market volatility. We assess possible concerns of bias and/or arbitrariness in selecting the prediction horizon by estimating the out-of-sample R^2 in a continuous time span of up to 110 days. The results still support that FRM with $\tau = 5\%$ has the highest average predictive ability within 110 days than others. To investigate whether FRM demonstrates superior predictive power for future market volatility in comparison to other risk measures, we further utilize eXtreme Gradient Boosting (XGBoost) to predict future market volatility based on the risk measures with 10 day lagged. To distinguish the contribution of different risk measures in a non-linear model (XGBoost), we further calculate their Shapley value (Lundberg and Lee 2017) for model explanation and find that FRM $\tau = 5\%$ contributes the most.

4.4. FRM's explanatory power for the sharpe ratio

According to Proposition 3.1, *FRM* is proportional to the spread between in-sample and true pricing kernel volatility. As such, due to the duality between pricing kernel volatility and the maximal attainable Sharpe ratio, it should be proportional to the sampling error of the Sharpe ratio and, therefore, to its volatility. To assess this, we explore the link between the *FRM@Crypto* index and the volatility of the Sharpe ratio for each crypto currency by estimating by Ordinary Least Squares (OLS) the following regression model:

$$\textit{Sharpe Ratio Volatility}_{i,t} = \theta_0 FRM_{t-l} + \textit{Controls} + \alpha_i + \varepsilon_{i,t} \tag{36}$$

Here, $\textit{Sharpe Ratio Volatility}_{i,t}$ represents crypto i's Sharpe ratio volatility over the previous 63 trading days relative to time t. FRM_{t-l} is the *FRM@Crypto* index at time $t-l$, and we set $l = 0$, $l = 10$, $l = 25$, $l = 110$ to test for a predictive relationship on a contemporaneous basis and with a lag of 10 days, 5 weeks, and 5 months, respectively. *Controls* are variables that reflect the time trend, different currencies' market values at $t-1$, and macro features at $t-1$. To be more specific, the macro features include the US dollar index, yield level in USD, VIX, CVIX, S&P 500 index. α_i is the fixed effects for each crypto currency. If Remark 3.1 works, we assume θ_0 is positive.

Table 6 shows the estimated effects of *FRM@Crypto* on the volatility of the Sharpe ratio. These findings link increases in *FRM@Crypto* and heightened Sharpe ratio volatility, and validate the posited connection between these two variables. This relationship remains consistent across various τ levels when calculating *FRM@Crypto* as well as with different lags of the *FRM@Crypto* index.

4.5. Application of FRM in portfolio construction

We initiate portfolio construction using the Markowitz framework, or mean-variance (MV) rule. Specifically, we minimize risk, as measured by variance, for a given level of return. Following this, we evaluate the out-of-sample predictive ability of risk measures for the optimized portfolio's volatility for future 10-day, 5-week, and 5-month periods to test whether FRM has the best predictive power. The portfolio construction methodology is outlined as follows:

Consider N coins with a vector of expected returns μ, and covariance matrix (Σ). The problem is to define the optimal portfolio weights vector w, which minimizes the portfolio variance subject to $w^\top \mathbf{1}_N = 1$, where $\mathbf{1}_N$ represents a column vector with the size N whose components are equivalent to

Table 6. *FRM@Crypto*'s explanatory power for Sharpe ratio's volatility.

	FRM 5%	FRM 25%	FRM 50%
	$l = 0$		
θ_0	0.0908***	0.2838***	0.1211***
Standard Error	0.009	0.020	0.012
Adjusted R-squared	0.245	0.247	0.245
Controls	YES	YES	YES
Crypto FE	YES	YES	YES
Obs	26,264	26,264	26,264
	$l = 10$		
θ_0	0.0850***	0.2716***	0.1126***
Standard Error	0.009	0.020	0.011
Adjusted R-squared	0.248	0.250	0.248
Controls	YES	YES	YES
Crypto FE	YES	YES	YES
Obs	25,989	25,989	25,989
	$l = 25$		
θ_0	0.0748***	0.2629***	0.1059***
Standard Error	0.010	0.023	0.013
Adjusted R-squared	0.269	0.272	0.270
Controls	YES	YES	YES
Crypto FE	YES	YES	YES
Obs	21,924	21,924	21,924
	$l = 63$		
θ_0	0.0981***	0.3129***	0.1310***
Standard Error	0.012	0.027	0.015
Adjusted R-squared	0.284	0.287	0.285
Controls	YES	YES	YES
Crypto FE	YES	YES	YES
Obs	16,280	16,280	16,280
	$l = 110$		
θ_0	0.1040***	0.3501***	0.1401***
Standard Error	0.017	0.035	0.020
Adjusted R-squared	0.149	0.154	0.150
Controls	YES	YES	YES
Crypto FE	YES	YES	YES
Obs	10,229	10,229	10,229

Note: ***, **, * denote significance at 1%, 5%, 10% level. The control variables consist of a time trend, different cryptos' market value and the macro variables of $t-1$ period. The sample period is 1 June 2015 to 31 May 2022.

one (Markowitz 1959). The MV portfolio can be obtained by solving the following optimization problem:

$$\min_{w\in\mathbb{R}^p} \quad w^\top \Sigma w \qquad \text{s.t.} \quad x^\top w \geq \mu, \quad w^\top \mathbf{1}_N = 1 \tag{37}$$

Here, $w = (w_1, w_2, \ldots, w_N)^\top$ are the weights of N coins, and x is the $(N \times 1)$ vector of their mean returns.

The problem in equation (37) is solved sequentially for a rolling window of data of fixed length. Specifically we set the window size s to 120 days. We adopt daily re-balancing, hence

Table 7. Out-of-sample predictive ability of risk measures for volatility of MV portfolio.

RHS	10 days	5 weeks	3 months	5 months
FRM 5%	0.801	0.646	0.836	0.687
FRM 25%	0.742	0.632	0.747	0.597
FRM 50%	0.735	0.630	0.741	0.618
Bayesian Graphical VAR	0.724	0.740	0.771	0.641
Granger Causality	0.671	0.624	0.610	0.647
Principal Components	0.677	0.760	0.712	0.777
Total Connectedness	0.630	0.557	0.855	0.498

rolling the window by one day at a time. On each rebalancing day, we use the data of the previous 120 days to estimate the weight w for the portfolio strategy, and use this information to calculate the weighted return on the day after rebalancing. The out-of-sample cumulative wealth (W) is calculated as below:

$$\begin{aligned} W_{t+1} &= W_t + R_t^{Portfolio} \\ &= W_t + \hat{w}_t^\top X_{t+1} \end{aligned} \tag{38}$$

Here, $R_t^{Portfolio}$ represents the portfolio's daily return on day t, while X_{t+1} is the vector of coins' returns on day $t+1$, $X_{t+1} = (r_{1t+1}, r_{2t+1}, \ldots, r_{Nt+1})^\top$. The initial value of W is set to \$1. The variable w_t denotes the vector of weights of the coins, representing the solution of equation (37) based on the sample from day $t-119$ to day t.

We then employ equations (33) to (35) to assess and compare the out-of-sample predictive capabilities of FRM and other risk measures for the volatility of the portfolio constructed using the MV rule. The results are presented in table 7, where FRM with $\tau = 5\%$ demonstrates the highest prediction power.

To further assess whether the FRM indicator enhances portfolio performance, we also employ FRM to construct two Tail Event Comovement (TEC) portfolios (Ren *et al.* 2022). The concept of a TEC portfolio is to minimize tail risk comovement or joint tail events for a specified level of returns. Considering λ_j as an indicator of tail risk for crypto j, the natural approach is to minimize the value across all cryptocurrencies. Consequently, a Linear Tail Event Comovement (LTEC) portfolio method can be developed:

$$\min_{w\in\mathbb{R}^p} \quad \lambda^\top w \qquad \text{s.t.} \quad x^\top w \geq \mu, \quad w^\top \mathbf{1}_N = 1 \tag{39}$$

where $\lambda = (\lambda_1, \lambda_2, \ldots, \lambda_N)^\top$ denotes joint tail events.

The second TEC approach is to construct Quadratic Tail Event Co-movement (QTEC) portfolios,

$$\min_{w\in\mathbb{R}^p} \quad \gamma w^\top \Sigma_\lambda w + (1-\gamma)\lambda^\top w \qquad \text{s.t.} \quad x^\top w \geq \mu, \quad w^\top \mathbf{1}_N = 1 \tag{40}$$

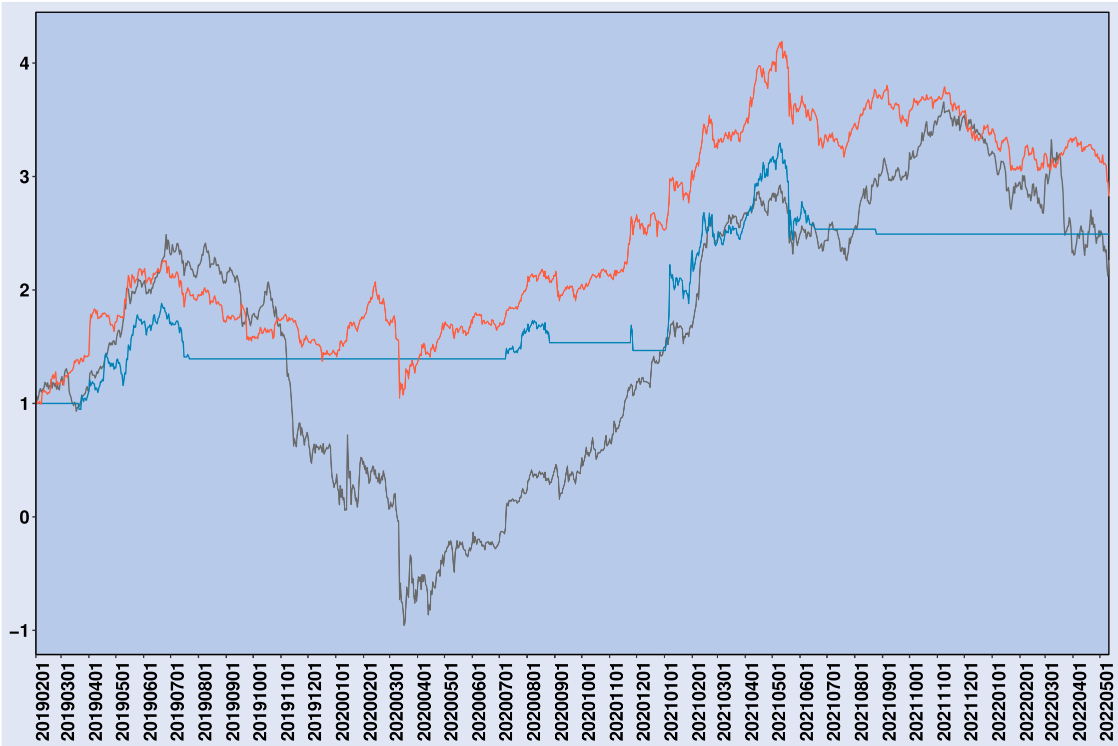

Figure 3. Cumulative wealth of MV, QTEC and LTEC (FRM with $\tau = 0.05$ and $\gamma = 0.8$).

Table 8. Portfolio performance based on mean-variance (MV) rule, TEC and QTEC.

Methodology	Cumulative Return	Annualized Daily Return	Annualized Volatility of Return	Annualized Sharpe Ratio
QTEC	1.825	0.203	0.355	0.572
MV	1.262	0.074	10.711	0.007
LTEC	1.492	0.131	0.295	0.444

Note: Annualized Daily Return is calculated as $\textit{Cumulative Return}^{\frac{1}{3.25}} - 1$Annualized Volatility of Return is calculated as $\sqrt{252} \times$ *Standard Deviation of Daily Return*Annualized Sharpe Ratio is calculated as $\frac{\textit{Annualized Daily Return}}{\textit{Annualized Volatility of Return}}$.

with Σ_λ the covariance matrix of λ; γ denotes the scale parameter between 0 and 1. If $\gamma = 0$, the QTEC portfolio turns to LTEC portfolio.

The portfolio wealth based on MV, LTEC, and QTEC are shown in figure 3. To compare their distinctions, we report the accumulated return, average daily return, volatility of daily return, and Sharpe ratio in table 8. Our findings indicate that both the QTEC and LTEC portfolio approaches exhibit higher returns and Sharpe ratios, accompanied by lower volatility compared to MV methodologies. This provides evidence that the inclusion of FRM enhances portfolio construction.

5. Risk contagion in tail-event network

For each trading day, the quantile LASSO regression coefficients from equation (1) can be arranged into an $N \times N$ adjacency matrix $A = \{\beta_{i,j}\}$, where $\beta_{i,i} = 0$ and N represent the number of cryptocurrencies. Based on graph theory, the adjacency matrix representation allows us to detect the TE risk interaction between the selected cryptocurrencies. The adjacency matrix can be denoted as:

$$A = \begin{pmatrix} 0 & \beta_{1,2} & \cdots & \beta_{1,N} \\ \beta_{2,1} & 0 & \cdots & \beta_{2,N} \\ \vdots & \vdots & \ddots & \vdots \\ \beta_{N,1} & \beta_{N,2} & \cdots & 0 \end{pmatrix} \tag{41}$$

Consider a network $G = \{N, \omega\}$, constituted by a set of links ω that connecting pairs of nodes and a set of nodes $n = 1, 2, \ldots, n$. If there is a connection between two nodes i and j, we denote it as $(i,j) \in \omega$.

Figure 4 displays graph representation on 4 July, 2021 for 15 coins. The lines that are highlighted are the incoming and outgoing links for Bitcoin, and the node size is proportional to $\lambda_{j,t}$.

To further explore the tail-event contagion between different coins, we calculate different centrality indexes to quantify the average importance of nodes within a network or graph.

Eigenvector centrality

According to the definition of Bonacich (1987), eigenvector centrality measures the importance of a node in a network

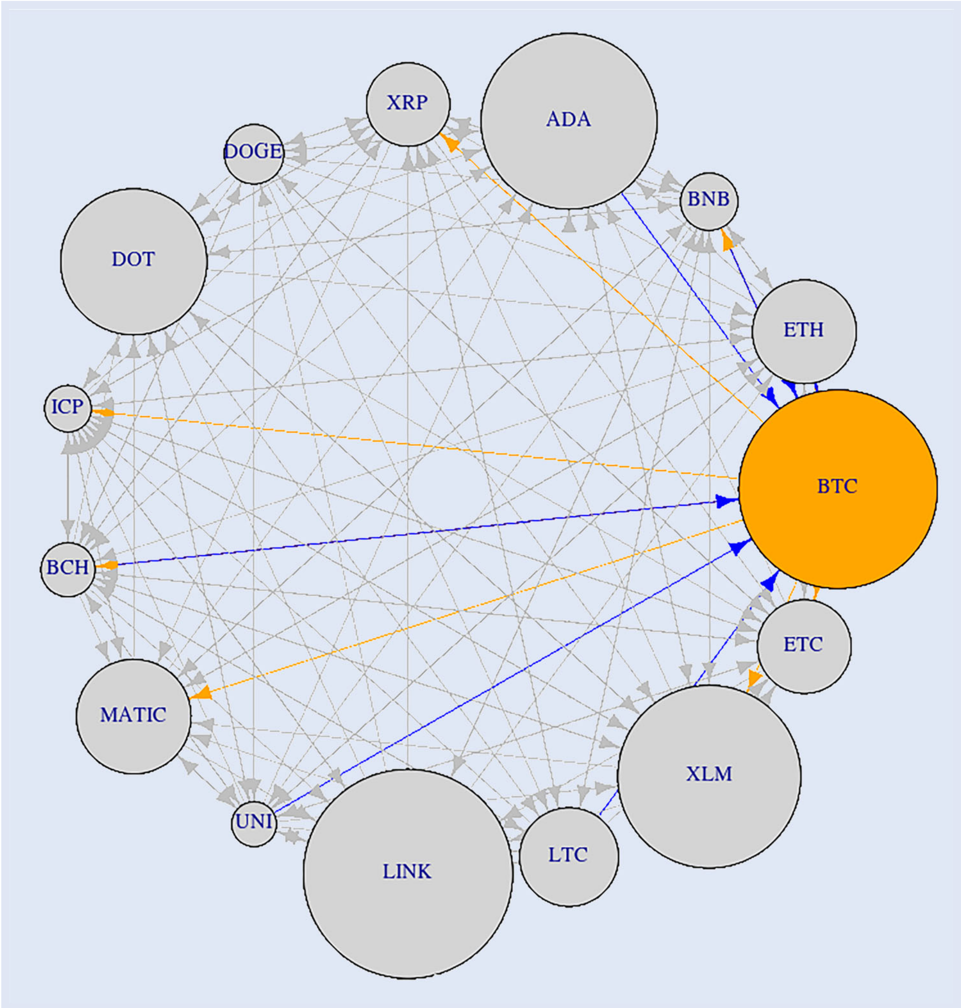

Figure 4. Network representation of FRM@Crypto for 4 July 2021.

based on its connections to other important nodes in the network. In other words, a node is considered important if it is connected to other nodes that are also important.

We could express the adjacency matrix (A) as:

$$A * v = \delta v \tag{42}$$

where δ is the largest eigenvalue and v denotes the eigenvector which corresponds to the centrality scores of the nodes in the network. On each trading day, the eigenvector centrality score of node i (v_i) and the eigenvector centrality index *EG Index* for the crypto market are computed as follows:

$$v_i = \delta^{-1} \sum_{j \neq i} \beta_{ij} v_j, \quad EG\ Index = \frac{1}{N} \sum_{i=1}^{N} v_i \tag{43}$$

In equation (43), centrality score of a node i is proportional to the sum of the centrality scores of its neighbors, weighted by the strength of the connections between them. A large value of v_i means that the node i is highly central, implying that node i is linked either to several other nodes or is linked to a few highly central nodes.

Closeness centrality

Closeness is a measure of centrality that was originally proposed by Freeman (1978). It focuses on the distance between one node and all other nodes in the network, and can be interpreted as the time it takes for information to spread from one node to another. Specifically, the closeness of a given node i and the market's closeness centrality index (*CC Index*) on each trading day are defined as follows:

$$CC_i = \sum_{i=1}^{N} \frac{1}{d_{(i,j)}}, \quad CC\ Index = \frac{1}{N} \sum_{i=1}^{N} CC_i \tag{44}$$

where $d_{(i,j)}$ measure the distance between a node i and another node j in the network (Ben Amor *et al.* 2022).

We conducted a comparison between *FRM@Crypto* and the two centrality indices, namely closeness index and eigenvector centrality (Billio *et al.* 2012). Figure 5(a,b) depicts the time series trend of these indices, and table 9 presents the correlation between *FRM@Crypto* and the centrality indices. As the number of non-zero β_{ij} in the adjacency matrix (see equation (41)) decreases, the TE risk spillover channels are concentrated within a minimal number of cryptocurrencies, and the links between these coins also reduce drastically. In this situation, we observe a decline in the closeness index, but an increase in *FRM@Crypto*, indicating a serious market risk. However, eigenvector centrality showed a positive relationship with *FRM@Crypto*. This is because eigenvector centrality measures the importance of a node in

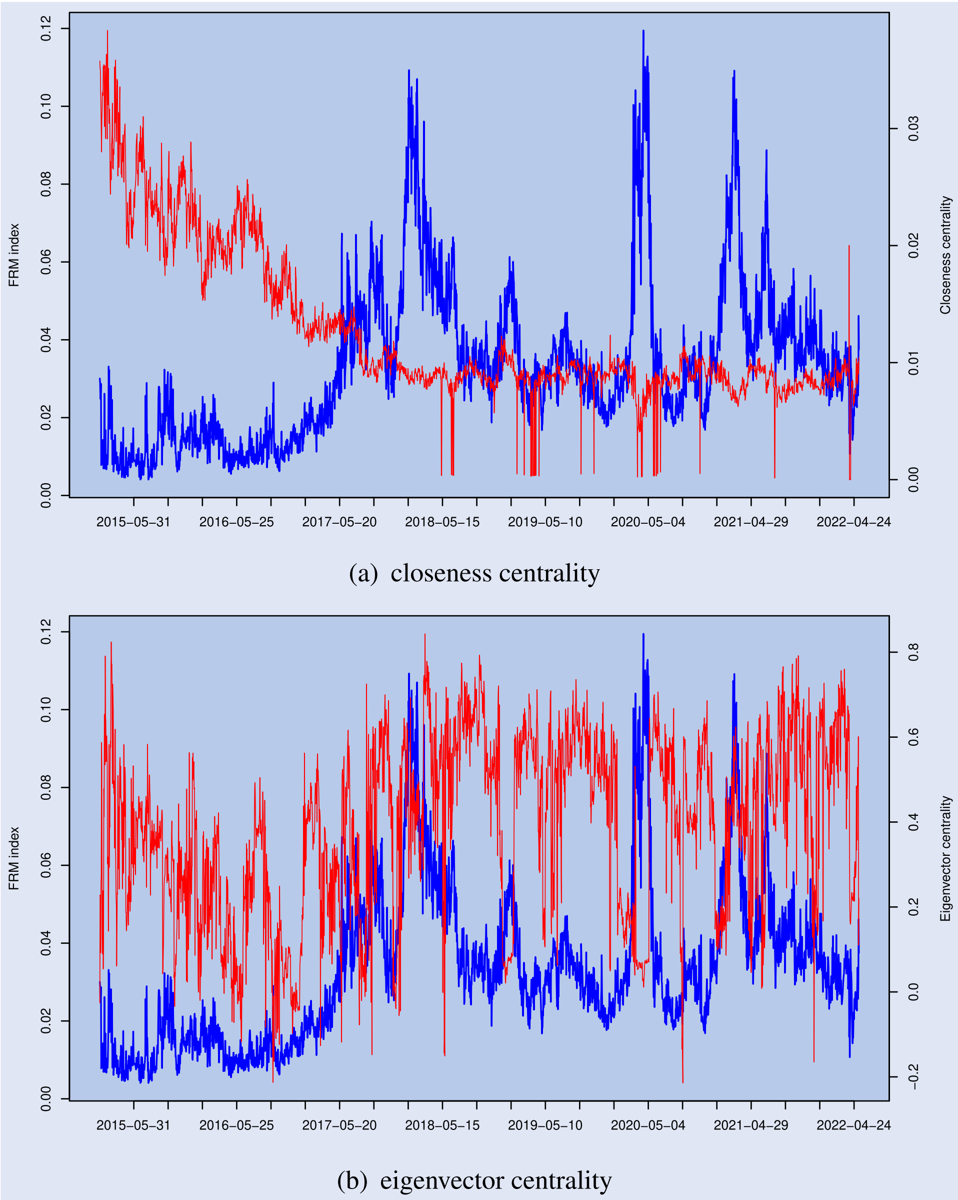

(a) closeness centrality

(b) eigenvector centrality

Figure 5. 5% *FRM@Crypto* and centrality index (a) closeness centrality (b) eigenvector centrality.

Table 9. Pearson test results of *FRM@Crypto* and centrality indexes.

	FRM	Closeness centrality	Eigenvector centrality
FRM		− 0.602***	0.156***
Closeness centrality	− 0.602***		− 0.310***
Eigenvector centrality	0.156***	− 0.310***	

Note: ***, **, * denote significance at 1%, 5%, 10% level.

a network by assigning relative scores based on how connected they are to the central node in the TE risk contagion network. When the systemic TE risks concentrate in a few coins, the influential impacts of these core coin also increase significantly, which could trigger the rise of the average eigenvector centrality. We also compare FRM's relationship with other centrality index in Appendix A.3, *FRM@Crypto* still maintains a significant association with these centrality indexes.

6. Conclusions

This paper extends the existing literature on FRM by providing a deeper economic interpretation of the FRM risk index. In the theoretical section, we first analyze the FRM index as a Lagrangian multiplier, representing a 'shadow price' that reflects the marginal gain (in terms of fit) achieved by relaxing the constraint on model parameters. Furthermore, we show that the penalized term in Quantile LASSO is directly linked to the difference between estimated mean returns derived from in-sample and pseudo-out-of-sample cross-validation methods. We use this to establish that FRM has a positive correlation with the volatility of asset return, as well as with the discrepancy between the in-sample estimations and the true (but unobservable) volatilities of the pricing kernel and maximal Sharpe ratios.

In the empirical section, this study explores the interdependencies among tail events (TE) within cryptocurrency markets while introducing an innovative market risk measure using the

FRM framework. Confirming the characteristics of FRM outlined in the theoretical section, we find a strong correlation between *FRM@Crypto* and CRIX volatility. Additionally, we assess the predictive ability of *FRM@Crypto* for future market volatility and compare its efficacy against other commonly used risk measures. Our findings indicate that *FRM@Crypto* demonstrates superior predictive performance compared to other risk measures over short-term horizons. The empirical findings demonstrating *FRM@Crypto*'s ability to explain Sharpe ratio volatility further reinforce the empirical support for the theoretical properties of FRM that we have derived. In addition, we integrate FRM in a Markowitz-type framework to construct tail event comovement portfolios, and show that this new portfolio attains significant improvements in Sharpe ratio as well as return. Furthermore, by examining the tail-event network created from the coefficients of the Quantile LASSO, we discover varying correlations between FRM and different centrality indices. Our findings strongly support the notion that *FRM@Crypto* carries valuable forward-looking information about risk in crypto markets.

Disclosure statement

No potential conflict of interest was reported by the author(s).

Funding

This work was supported by innovation program "FINTECH: A Financial supervision and Technology compliance training program" under Grant 825215; the Czech Science Foundation under Grant 19-28231X; "IDA Institute for Digital Assets", CF166/15.11.2022, contract number 760046/23.05.2023, financed under the Romania's National Recovery and Resilience Plan, Apel nr. PNRR-III-C9-2022-I8.; the National Natural Science Foundation of China under Grant 72302237; China Postdoctoral Science Foundation (2023M743984); Guangdong Basic and Applied Basic Research Foundation (2024A1515010314).

References

Adrian, T. and Brunnermeier, M.K., CoVaR. *Am. Econ. Rev.*, 2016, **106**, 1705–1741.

Ahelegbey, D.F., Billio, M. and Casarin, R., Bayesian graphical models for structural vector autoregressive processes. *J. Appl. Econom.*, 2016, **31**, 357–386.

Ahelegbey, D.F., Giudici, P. and Mojtahedi, F., Tail risk measurement in crypto-asset markets. *Int. Rev. Financial Anal.*, 2021, **73**, 101604.

Bahadur, R.R., A note on quantiles in large samples. *Ann. Math. Statist.*, 1966, **37**, 577–580.

Ben Amor, S., Althof, M. and Härdle, W.K., FRM financial risk meter for emerging markets. *Res. Int. Business Finance*, 2022, **60**, 101594.

Billio, M., Getmansky, M., Lo, A.W. and Pelizzon, L., Econometric measures of connectedness and systemic risk in the finance and insurance sectors. *J. Financ. Econ.*, 2012, **104**, 535–559.

Bonacich, P., Power and centrality: A family of measures. *Am. J. Sociol.*, 1987, **92**, 1170–1182.

Borri, N., Conditional tail-risk in cryptocurrency markets. *J. Empirical Finance*, 2019, **50**, 1–19.

Campbell, J.Y. and Thompson, S.B., Predicting excess stock returns out of sample: Can anything beat the historical average? *Rev. Financ. Stud.*, 2008, **21**, 1509–1531.

Chen, T. and Guestrin, C., Xgboost: A scalable tree boosting system. In *Proceedings of the 22nd ACM SIGKDD International Conference on Knowledge Discovery and Data Mining*, pp. 785–794, 2016.

Chen, Y. and Potì, V., Econometric identification of the attainable maximal sharpe ratio by optimal shrinkage of the cross-section of asset returns. *Econ. Lett.*, 2024, **235**, 111531.

Cochrane, J., *Asset Pricing*, 2009 (Princeton University Press).

Diebold, F.X. and Yilmaz, K., Better to give than to receive: Predictive directional measurement of volatility spillovers. *Int. J. Forecast.*, 2012, **28**, 57–66.

Engle, R.F. and Kroner, K.F., Multivariate simultaneous generalized ARCH. *Econ. Theory.*, 1995, **11**, 122–150.

Fan, Y., Härdle, W.K., Wang, W. and Zhu, L., Single-Index-Based CoVaR with very high-dimensional covariates. *J. Bus. Econ. Statist.*, 2018, **36**, 212–226.

Feng, W., Wang, Y. and Zhang, Z., Can cryptocurrencies be a safe haven: A tail risk perspective analysis. *Appl. Econ.*, 2018, **50**, 4745–4762.

Freeman, L.C., Centrality in social networks conceptual clarification. *Soc. Networks.*, 1978, **1**, 215–239.

Giudici, P., Hadji-Misheva, B. and Spelta, A., Network based scoring models to improve credit risk management in peer to peer lending platforms. *Frontiers Artif. Intell.*, 2019, **2**, 3.

Giudici, P., Leach, T. and Pagnottoni, P., Libra or Librae? Basket based stablecoins to mitigate foreign exchange volatility spillovers. *Finance Res. Lett.*, 2022, **44**, 102054.

Härdle, W.K., Wang, W. and Yu, L., TENET: Tail-Event driven network risk. *J. Econom.*, 2016, **192**, 499–513.

Hansen, L.P. and Jagannathan, R., Implications of security market data for models of dynamic economies. *J. Political Econ.*, 1991, **99**, 225–262.

Huang, D. and Zhou, G., Upper bounds on return predictability. *J. Financial Quant. Anal.*, 2017, **52**, 401–425.

Jiang, W., Xu, Q. and Zhang, R., Tail-event driven network of cryptocurrencies and conventional assets. *Finance Res. Lett.*, 2022, **46**, 102424.

Kirby, C., The restrictions on predictability implied by rational asset pricing models. *Rev. Financ. Stud.*, 1998, **11**, 343–382.

Klein, T., Thu, H.P. and Walther, T., Bitcoin is not the new gold–a comparison of volatility, correlation, and portfolio performance. *Int. Rev. Financial Anal.*, 2018, **59**, 105–116.

Korsaye, S.A., Quaini, A. and Trojani, F., Smart stochastic discount factors. Swiss Finance Institute Research Paper No. 21-51, 2021.

Kozak, S., Nagel, S. and Santosh, S., Shrinking the cross-section. *J. Financ. Econ.*, 2020, **135**, 271–292.

Liu, Y. and Just, A., *SHAPforxgboost: SHAP Plots for 'XGBoost'* R package version 0.1.0, 2020.

Lundberg, S.M. and Lee, S.I., A Unified Approach to Interpreting Model Predictions. In *Advances in Neural Information Processing Systems*, Vol. 30, 2017.

Markowitz, H., *Portfolio Selection*, 1959 (Yale University Press: New Haven, CT).

Mihoci, A., Althof, M., Chen, C.Y.H. and Härdle, W.K., FRM financial risk meter. In *The Econometrics of Networks*, Vol. 42 of *Advances in Econometrics*, pp. 335–368, 2020 (Emerald Group Publishing Limited).

Potì, V., A new tight and general bound on return predictability. *Econ. Lett.*, 2018, **162**, 140–145.

Potì, V. and Wang, D., The coskewness puzzle. *J. Bank. Finance*, 2010, **34**, 1827–1838.

Ren, R., Althof, M. and Härdle, W.K., Financial risk meter for cryptocurrencies and tail risk network-based portfolio construction. *Singapore Econ. Rev.*, 2022, 1–27. DOI: 10.1142/S0217590822480010.

Ren, R., Lu, M.J., Li, Y. and Härdle, W.K., Financial risk meter FRM based on expectiles. *J. Multivar. Anal.*, 2022, **189**, 104881.
Shahzad, S.J.H., Bouri, E., Roubaud, D. and Kristoufek, L., Safe haven, hedge and diversification for G7 stock markets: Gold versus Bitcoin. *Econ. Modell.*, 2020, **87**, 212–224.
Shahzad, S.J.H., Bouri, E., Roubaud, D., Kristoufek, L. and Lucey, B., Is Bitcoin a better safe-haven investment than gold and commodities?. *Int. Rev. Financial Anal.*, 2019, **63**, 322–330.
Shapley, L.S., A value for n-person games. In *Contributions to the Theory of Games (AM-28)*, *Volume II*, edited by H.W. Kuhn and A.W. Tucker, pp. 307–318, 1953 (Princeton University Press: Princeton). DOI: 10.1515/9781400881970-018.
Tibshirani, R., Regression shrinkage and selection via the Lasso. *J. Royal Statist. Soci.*, 1996, **58**, 267–288.
Trimborn, S. and Härdle, W.K., CRIX an index for cryptocurrencies. *J. Empirical Finance*, 2018, **49**, 107–122.
Wang, R., Althof, M. and Härdle, W.K., A financial risk meter for China. *Emerging Markets Rev.*, 2023, **56**, 101052.
Yu, L., Härdle, W.K., Borke, L. and Benschop, T., An AI approach to measuring financial risk. *Singapore Econ. Rev.*, 2019, **68**, 1529–1549.
Zbonakova, L., Härdle, W.K. and Wang, W., Time varying quantile Lasso. In *Applied Quantitative Finance*, Chap. 17, 2017 (Springer).

Appendices

Appendix 1. Additional mathematical proofs

A.1. Quantile regression as weighted linear regression

In this section we show that quantile regression is a special case of weighted least squares (WLS), which is an extension of OLS regression for the class of linear predictors. Thus, results for WLS regression will apply to quantile regression too. The WLS optimization problem for the sample size n with true parameter β_0 is as follows:

$$\widehat{\beta}_n = \arg\min_{\beta} \sum_i w_i (y_i - x_i^\top \beta)^2 = \left(\sum_i w_i x_i x_i^\top\right)^{-1} \sum_i w_i x_i y_i$$
$$= \sum_i \tilde{w}_i y_i = \sum_i \tilde{w}_i x_i^\top \beta_0 + \sum_i \tilde{w}_i \varepsilon_i = \beta_0 + \sum_i \tilde{w}_i \varepsilon_i \qquad \text{(A1)}$$

Here, $\tilde{w}_i = (\sum_i w_i x_i x_i^\top)^{-1} \sum_i w_i x_i$ so that $\sum_i \tilde{w}_i x_i^\top = (\sum_i w_i x_i x_i^\top)^{-1} \sum_i w_i x_i x_i^\top = I_n$, where I_n is an identity matrix conformable to β_0. Now, pre-multiply each side of equation (A1) by $x^\top$ to obtain the sample WLS conditional mean

$$x^\top \hat{\beta}_n = x^\top \beta_0 + x^\top \sum_i \tilde{w}_i \varepsilon_i \qquad \text{(A2)}$$

Next, note that, according to the Bahadur expansion for sample conditional quantiles, see Bahadur (1966), the following representation holds

$$\hat{Q}_{\tau,n}(x) = Q_\tau(x) + \frac{\tau - F_{Y\,|\,X,n}\{Q_\tau(x)\,|\,x\}}{f_{Y\,|\,X}\{Q_\tau(x)\,|\,x\}} + \mathcal{O}_{\mathrm{P}}(R_n) \qquad \text{(A3)}$$

Here, $Q_\tau(x) = x^\top \beta_\tau$ is the theoretical conditional quantile, $R_n = n^{-3/4}(\log n)^{3/2}$ and the density $f_{Y|X}$ is assumed to be twice differentiable. Expressing the above in terms of the empirical conditional cumulative distribution function , equation (A3) becomes

$$\hat{Q}_{\tau,n}(x) = Q_\tau(x) + n^{-1} \sum_i \frac{\tau - \mathbf{1}_{\{x_i = x\}} \mathbf{1}_{\{y_i \le Q_\tau(x_i)\}}}{f_{Y\,|\,X}\{q_\tau(x)\,|\,x\}} + \mathcal{O}_{\mathrm{P}}(R_n) \qquad \text{(A4)}$$

Now, compare the expression for the sample WLS conditional mean in equation (A2) with the sample conditional quantile in equation (A4). This comparison clarifies that we can obtain asymptotic equivalence of the conditional quantile estimator with the WLS estimator, or the equivalence between $\widehat{Q}_{\tau,n}(x) = x^\top \widehat{\beta}_{\tau,n}$ in equation (A4) and $x^\top \widehat{\beta}_n$ in equation (A2), by choosing the WLS weights w_i such that, $\forall x$,

$$x^\top \left(\sum_i \tilde{w}_i(w_i) \varepsilon_i \right) = \sum_i \frac{\tau - \mathbf{1}_{\{x_i = x\}} \mathbf{1}_{\{y_i \le q_\tau(x_i)\}}}{n f_{Y\,|\,X}\{q_\tau(x)\,|\,x\}}$$

That is, the conditional quantile regression is a special case of infeasible WLS for the above choice of WLS weights. Comparing equations (2) with (A1), we see that the unfeasible weights must be

$$w_i = \frac{\rho(y_i - x_i^\top \beta_0)}{(y_i - x_i^\top \beta_0)^2} \qquad \text{(A5)}$$

With this WLS view of quantile regression, Proposition 3.1 can be extended from the OLS optimization objective to the case of quantile loss, with the same ℓ_1 constraint.

A.2. Mathematical explanation of $\mathrm{E}^{\mathrm{P}}[r_{t+1,k}]$

$\mathsf{E}^{\mathrm{P}}[r_{t+1,k}]$ can be written as:

$$\mathsf{E}^{\mathrm{P}}[r_{j,t+1}] \stackrel{\text{def}}{=} \mathsf{E}^{\mathrm{P}}\left[\mathsf{E}^{\mathrm{P}}[r_{j,t+1}\,|\,\mathcal{F}_t]\right]$$
$$= \mathsf{E}^{\mathrm{P}}\left[\mathsf{E}^{\mathrm{P}}[r_{j,t+1}\,|\,\mathsf{E}^{\mathrm{P}}_{\mathcal{F}_t}[r_{-j,t+1}], \mathcal{F}_t]\right] \qquad \text{(A6)}$$

where $\mathsf{E}^{\mathrm{P}}_{\mathcal{F}_t}[r_{-j,t+1}]$ denotes the conditional expectation for the (excess) return on all other assets except the k-th one.

If the data generating process of $r_{j,t+1}$ is strongly stationary, such that $\mathsf{E}^{\mathrm{P}}_{\mathcal{F}_t}[r_{j,t+1}]$ as constant for all t, or at least if the variation of $\mathsf{E}^{\mathrm{P}}_{\mathcal{F}_t}[r_{j,t+1}]$ is limited enough that we can treat it as constant for all t within the estimation window of FRM (the 62-day rolling estimation window in our case), then equation (A6) can be written as:

$$\mathsf{E}^{\mathrm{P}}\left[\mathsf{E}^{\mathrm{P}}[r_{j,t+1}\,|\,\mathsf{E}^{\mathrm{P}}_{\mathcal{F}_t}[r_{-j,t+1}], \mathcal{F}_t]\right] = \mathsf{E}^{\mathrm{P}}[r_{j,t+1}\,|\,r_{-j,t+1}, \mathcal{F}_t] \qquad \text{(A7)}$$

Based on equations (A6) and (A7), we then get:

$$\mathsf{E}^{\mathrm{P}}[r_{j,t+1}] = \mathsf{E}^{\mathrm{P}}[r_{j,t+1}|r_{-j,t+1}, \mathcal{F}_t] \qquad \text{(A8)}$$

The right-hand side of equation (A8) can be modeled as a risk-consistent estimate of the FRM regression outlined in equation (1). This estimate can be obtained using a LASSO estimation, with the parameters determined through the cross-validation methodology (as depicted in equation (5)). We denote such estimate as $\mathsf{E}_n{}^{\mathrm{CV}}[r_{j,t+1}]$.

A.3. FRM and the spread between in- and out-of-sample predictability

For linear LASSO under the penalized regression formulation, the solution $\widehat{\beta}(\lambda_j)$ to the Lagrangian dual function $g(\lambda_j)$ for a fixed λ_j satisfies the equation (Mihoci *et al.* 2020):

$$\lambda_j = \frac{\hat{\varepsilon}^\top A_j \widehat{\beta}_j(\lambda_j)}{\|\,\widehat{\beta}_j(\lambda_j)\,\|_1} = \frac{\hat{\varepsilon}^\top \widehat{r}_j(\lambda_j)}{\|\,\widehat{\beta}_j(\lambda_j)\,\|_1} \propto \widehat{\mathsf{E}}^{\mathrm{P}}(\hat{\varepsilon}) \qquad \text{(A9)}$$

Here, $\varepsilon \in \mathbb{R}$ and $\widehat{\varepsilon} = (\hat{\varepsilon}_1, \ldots, \hat{\varepsilon}_T)^\top$ are theoretical (population) and sample errors for the linear regression model, hence for the regression without penalization. Only if $\lambda_j = 0$, $\widehat{\beta}_j(\lambda_j)$ is the OLS estimate of β_j and the sample mean of residuals to zero ($\widehat{\mathsf{E}}^{\mathrm{P}}(\hat{\varepsilon}) = 0$). Thus, λ_j reflects the difference between estimates of the mean return based on (in-sample) OLS and estimates based on pseudo-out-of-sample cross-validation (GACV).

Appendix 2. Alternative risk predictors

In this sector, we describe the four popular indicators/risk predictors with which we compare FRM.

(1) The *Bayesian graphical VAR index* is calculated based on the coefficient matrix of Bayesian graphical VAR (Ahelegbey *et al.* 2016). The index definition is as follows:

$$D = \sum_{i=1}^{N}\sum_{j=1}^{N} \mathbf{1}(\beta_{i,j})/N^2$$

$$\mathbf{1}(\beta_{i,j}) = \begin{cases} 1 & \text{if } \beta_{i,j} \neq 0 \\ 0 & \text{if } \beta_{i,j} = 0 \end{cases}$$

where D is the Bayesian graphical VAR index on a trading day; N represents the total number of cryptocurrencies; j and i represent the specific cryptocurrency; $\beta_{j,i}$ is the structural coefficient.

(2) The *Granger causality index (GC)* is estimated using a VAR (vector autoregression) model, where the time series data for each node is used to estimate the causal relationships between the nodes. The resulting Granger causality index matrix provides a quantitative measure of the strength of the causal relationships between nodes in the network. Following Billio *et al.* (2012), this index is defined as:

$$GC = \frac{1}{N(N-1)}\sum_{i=1}^{N}\sum_{j\neq i}^{N}(j \to i)$$

$$(j \to i) = \begin{cases} 1 & \text{if } j \text{ Granger causes } i \\ 0 & \text{Otherwise} \end{cases}$$

(3) The *principal components index* is the first principal component of the variance-covariance matrix of the cryptocurrencies' returns, and we construct this indicator based on Billio *et al.* (2012). The period when few principal components explain a larger percentage of total variation are associated with an increased interconnectedness between cryptocurrencies.

(4) The *total connectedness index* (*TCI*) measures the total connectedness or spillover effects among all markets in the system based on the forecast error variance decomposition (FEVD) matrices. Following Diebold and Yilmaz (2012), we construct it as follows:

$$TCI(H) = \frac{1}{H}\sum_{h=1}^{H}\sum_{i=1}^{p}|FEVD_i(h)| \tag{A10}$$

$$FEVD_i(h) = \frac{\sigma_i^2(h)}{\sigma^2(h)} \times 100 \tag{A11}$$

$$\sigma_i^2(h) = \mathrm{VAR}(e_{i,t+h} \mid \mathbf{y}_t) \tag{A12}$$

where $FEVD_i(h)$ is the forecast error variance decomposition matrix for cryptocurrency i at horizon h; $\sigma_i^2(h)$ is the variance of the forecast errors of cryptocurrency i's stock return at horizon $h = 200$, and $\sigma^2(h)$ is the total variance of the forecast errors of all assets at horizon h; $e_{i,t+h}$ is the forecast error of cryptocurrency i's stock return at horizon h and $\mathbf{y}_t$ is the vector of all cryptocurrencies' returns up to time t, which are estimated based on a VAR model.

Appendix 3. Alternative centrality indexes

To deepen the investigation into the robust relationship between FRM and centrality indexes, we compute three additional centrality indexes as suggested by Klein *et al.* (2018) and Ahelegbey *et al.* (2021) – Extreme Downside Correlation (EDC), Extreme Downside Hedge (EDH), and BEKK-GARCH – with the aim of exploring their correlation with FRM.

(1) *EDC centrality index*

EDC is a correlation-based method that assesses the marginal association between a pair of continuous variables, emphasizing the tail of their joint return distributions.

Let r_i represent the returns of coin i at time t, and let μ_i denote the historical mean of coin i. The EDC quantifies the tail correlation between coins i and j as follows:

$$EDC_{\tau,ij} = \frac{\sum_{t=1}^{T}[(r_{it}-\mu_i)_\tau (r_{jt}-\mu_j)_\tau]}{\sum_{t=1}^{T}[(r_{it}-\mu_i)_\tau^2]^{0.5}[(r_{jt}-\mu_j)_\tau^2]^{0.5}} \tag{A13}$$

where

$$(r_{it}-\mu_i)_\tau = \begin{cases} r_{it}-\mu_i & \text{if } r_{it} < r_{\tau i} = F_{r_i}^{-1}(\tau) \\ 0 & \text{Otherwise} \end{cases}$$

where $r_{\tau i}$ is the left-side τ-quantile of the standardized distribution on the coin's return r_i, and $F_{r_i}(\tau) = \Pr(r_i \leq \tau)$ is the cumulative distribution function (cdf) of r_i.

The EDC centrality index is defined as:

$$EDC_i = \sum_{j=1, j\neq i}^{N}\frac{1}{EDC_{\tau,ij}}, \quad EDC\ Index = \frac{1}{N}\sum_{i=1}^{N} EDC_i \tag{A14}$$

(2) *EDH centrality index*

EDH reflects the sensitivity of coin-i's return with respect to conditional value at risk $CVaR$ of coin j:

$$r_{it} = \alpha_i + \sum_{j=1, j\neq i}^{N}\beta_{i\mid j}\Delta CVaR_{jt} + \varepsilon_{it} \tag{A15}$$

where $\Delta CVaR_{jt} = CVaR_{jt} - CVaR_{jt-1}$.

The EDH centrality index is defined as:

$$EDH_i = \sum_{j=1, j\neq i}^{N}\frac{1}{\beta_{i\mid j}}, \quad EDH\ Index = \frac{1}{N}\sum_{i=1}^{N} EDH_i \tag{A16}$$

(3) *BEKK-GARCH centrality index*

The BEKK-GARCH model was initially developed by Engle and Kroner (1995). Let R_t be a N-dimemsional vector of coin return at time t, denoted as:

$$R_t = \mu_t + \varepsilon_t \tag{A17}$$

where μ_t is a N-dimensional conditional mean structure. For the N-dimensional vector ε_t, we assume $\varepsilon_t \mid \mathcal{F}_{t-1} \sim \mathrm{N}(0, H_t)$. ε_t can be expressed as:

$$\varepsilon_t = H_t^{\frac{1}{2}}\xi_t \tag{A18}$$

where H_t denotes the $(N \times N)$ – sized conditional variance matrix and ξ_t refers to a N-dimensional vector of standard normally distributed and i.i.d. random variables with zero mean and $\mathsf{E}(\xi_t, xi_t^\top) = \mathrm{I}_t$.

$$H_t = C^\top C + A^\top \varepsilon_{t-1}\varepsilon_{t-1}^\top A + G^\top H_{t-1} G \tag{A19}$$

where A, G, C are $N \times N$ parameter matrices and C is lower triangular. We use the information of G to construct centrality index.

Table A1. Robust test of correlation of *FRM@Crypto* and other centrality indices.

	EDC centrality	EDH centrality	BEKK-GARCH centrality
FRM	0.303***	0.314***	– 0.124***

Note: ***, **, * denote significance at 1%, 5%, 10% level.

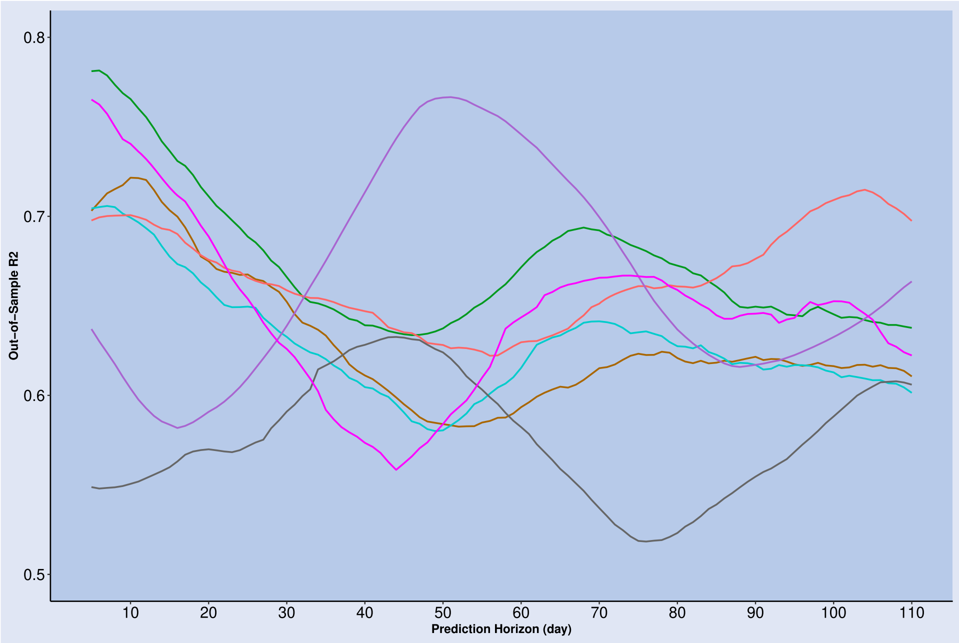

Figure A1. Dynamic out-of-sample R^2 of risk measures (The calculation process of out-of-sample R^2 is described in Section 4.3. FRM with $\tau = 5\%$, FRM with $\tau = 25\%$, FRM with $\tau = 50\%$, Bayesian Graphical VAR, Principal Components, Granger Causality, Total Connectedness).

Table A2. Mean value of risk measures' out-of-sample R^2 with 110 days forecasting horizon.

	FRM with $\tau = 5\%$	FRM with $\tau = 25\%$	FRM with $\tau = 50\%$	Bayesian Graphical VAR	Principal Components	Granger Causality	Total Connectedness
Mean Value	0.674	0.630	0.629	0.666	0.576	0.664	0.646

The BEKK-GARCH centrality index is defined as:

$$BEKK - GARCH\ Indicator_i = \sum_{j=1, j \neq i}^{N} \frac{1}{G_{i,j}},$$
$$BEKK - GARCH\ Index = \frac{1}{N} \sum_{i=1}^{N} G_i \quad \text{(A20)}$$

The Pearson corelation between FRM and the above three centrality index is shown in table A1. Our findings reveal a positive association between FRM and extreme downside centrality (EDC and EDH index), while displaying a negative correlation with the variance correlation among the coins. This outcome aligns with the characteristic of FRM, which focuses on capturing tail risk rather than correlation.

Appendix 4. Robust analysis for FRM's prediction power

A.4. Sensitivity to the selection of prediction horizon

The reason that we choose 10 days, 5 weeks, and 5 months as the lag parameter in the main part is to signify short-term, medium-term, and long-term horizons, respectively. In order to mitigate potential bias arising from parameter selection, we extend the horizon to encompass a continuous daily interval ranging from 5 day to 5 months (110 days). The out-of-sample R^2 at each prediction horizon of the risk measures is plotted in figure A1.

The findings indicate that FRM with $\tau = 5\%$ outperforms other indicators when the prediction horizon is within 32 days. Despite a decrease in the prediction ability of FRM with $\tau = 5\%$ as the horizon period increases, its mean value still surpasses that of other risk measures (see table A2).

A.5. FRM's prediction ability test based on non-linear model

To investigate whether FRM demonstrates superior predictive power for future market volatility in comparison to other risk measures, we utilize eXtreme Gradient Boosting (XGBoost), which is a robust and widely adopted machine learning algorithm within the ensemble learning methods.The XGBoost algorithm is a scalable boosting algorithm proposed by Chen and Guestrin (2016). It is an improved version of the gradient boosting decision tree, using boosting to iteratively learn multiple decision trees. To distinguish the contribution of different risk measures in a non-linear model (XGBoost), we further calculate their Shapley value (Lundberg and Lee 2017) for model explanation.

In XGBoost model, We use FRM with $\tau = 5\%$, $\tau = 25\%$, $\tau = 50\%$, Bayesian Graphical VAR index, the Principal Components index, the Degree of Granger Causality index, and the Total Connectedness index as the input of the algorithm to predict market volatilty. The algorithm is trained in a 62-day rolling window:

$$y_t^{\text{Market}} = \text{XGBoost}(x_{1t}, x_{2t}, \ldots, x_{kt}) + \varepsilon_t \quad \text{(A21)}$$

where y_t^{Market} represents the market volatility on day $t, x_{1t}, x_{2t}, \ldots, x_{kt}$ are the features that are used in predicting the market volatility. In our case, we use the risk measures. The XGBoost(.) is the XGBoost algorithm determined within a rolling window using historical data from the past 62 days. The prediction error ε_t is measured by the difference between the real value and the predicted value.

In addition to out-of-sample R^2 that we use in our main result, we utilize mean absolute error (MAE) and root mean square error

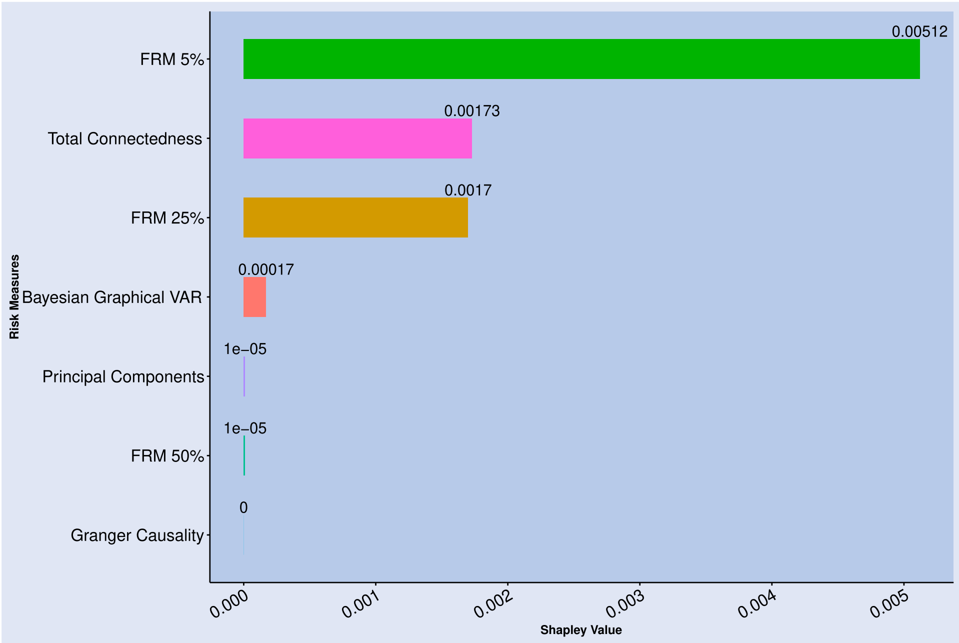

Figure A2. Shapley value of risk measures in explaining market volatility based on XGBoost methodology.

Table A3. Out-of-Sample predictive ability of risk measures for future market volatility based on XGBoost methodology.

$R^{oos}_{XGBoost}$	$MAE_{XGBoost}$	$RMSE_{XGBoost}$
0.929	0.002	0.004

(RMSE) to assess prediction accuracy. Table A3 demonstrates an out-of-sample R^2 of 0.929, accompanied by a MAE of 0.002 and an RMSE of 0.004. These results support the algorithm's robust predictive capabilities for market volatility.

The Shapley values were derived based on coalitional game theory (Shapley 1953) to explain machine learning model output by calculating the contribution of each feature to the model prediction results. The R package that we used in calculating Shapley value is called SHAP developed by Liu and Just (2020).

$$\hat{y}_t^{\text{Market}} = \hat{y}_{base} + f(x_{1t}) + f(x_{2t}) + \cdots + f(x_{kt}),$$

$$SHAP_k = \frac{\sum_{t=1}^{T} f(x_{kt})}{T}$$

where $\hat{y}_t^{\text{Market}}$ is the predicted value of market volatility; x_{kt} represents the feature k on day t ($t \in [1, T]$). $f(x_{kt})$ is the Shapley value of x_{kt}, which reflects the contribution of x_{kt} on the prediction. If $f(x_{kt}) > 0$, it indicates that this feature has a positive effect on the prediction results. Otherwise, the prediction results play a reverse role. We then calculate the mean value of the Shapley value in the whole time span as the kth risk measure's Shapley value.

Figure A2 reflects that the contribution of the FRM with $\tau = 5\%$(Shapley value: 0.00512) is more prominent than other risk measure in predicting future market volatility. FRM with $\tau = 25\%$ ranks the second. This result supports that FRM with smaller τ have better prediction power in market risk.